

A PRIMAL HYBRID FINITE ELEMENT METHOD TO SOLVE GENERAL COMPRESSIBLE, QUASI-INCOMPRESSIBLE AND INCOMPRESSIBLE ELASTICITY USING STABLE H(DIV)-L2 SPACES

**PHILIPPE R. B. DEVLOO¹, GIOVANE AVANCINI², NATHAN SHAUER³ AND HUGO
L. OLIVEIRA⁴**

¹ State University of Campinas, Faculty of Civil Engineering
Av. Albert Einstein, 901 - Cidade Universitária, Campinas - SP, 13083-852
phil@unicamp.br

² State University of Campinas, Faculty of Civil Engineering
Av. Albert Einstein, 901 - Cidade Universitária, Campinas - SP, 13083-852
giovanea@unicamp.br

³ State University of Campinas, Faculty of Civil Engineering
Av. Albert Einstein, 901 - Cidade Universitária, Campinas - SP, 13083-852
shauer@unicamp.br

⁴ State University of Campinas, Faculty of Civil Engineering
Av. Albert Einstein, 901 - Cidade Universitária, Campinas - SP, 13083-852
hluiiz@unicamp.br

Key words: Hybrid finite element method, incompressible elasticity, De Rham compatible spaces

Abstract. Hybrid methods are usually derived from an extended variational principle, in which the interelement continuity of the functions subspace is removed and weakly enforced by means of a Lagrange multiplier. In this context, a new primal hybrid finite element formulation is presented, which uses H(div) conforming displacement functions and discontinuous L2 approximation for pressure together with shear traction functions to weakly enforce tangential displacement. This combination allows the simulation of compressible, quasi-incompressible and fully incompressible elastic solids, with convergence rates independent of its bulk modulus. The proposed approach benefits from the property that the divergence of the H(div) displacement functions is De Rham compatible with the (dual) pressure functions. The hybridization of the tangential displacements is weakly enforced through a lower order shear stress space. This leads to a saddle-point problem that is stable over the full range of poisson coefficient (large compressibility up to incompressible). Moreover, a boundary stress (normal and shear) can be recovered that satisfies elementwise equilibrium. Hybridizing the tangent stresses and condensing the internal degrees of freedom, a positive-definite matrix with improved spectral properties can be recovered. The stability, consistency and local conservation features are discussed in details. The formulation is tested and verified for different test cases.

1 INTRODUCTION

In the context of linear elasticity, several numerical methods have been developed in the past years. The most used one is the Finite Element Method (FEM). Using a continuous Galerkin approach to approximate the displacements may lead to shear-locking phenomenon due to spurious energy modes under bending [1, 2] or volume-locking under quasi or full incompressibility, as the stresses go to infinity [3, 4].

There are different ways in the literature to overcome these drawbacks. One possible choice is to employ a mixed formulation [5, 6] where the displacements and the stresses (or pressure) are approximated independently - i.e. the Taylor Hood elements [7] fulfill the *inf-sup* condition yielding stable results for incompressible regime. This kind of approximation, on the other hand, is not locally conservative as it does not satisfy the divergence constraint in a strong manner. Another possibility is to use hybrid methods [] where the interelement continuity of a given field is broken and weakly imposed by means of a Lagrange multiplier (see for instance [8, 9, 10]).

In this work we extend the semi-hybrid approach proposed in [11] for Stokes problems to develop a new primal hybrid finite element formulation for elasticity based on a De Rham compatible pair $H(\text{div}) - L^2$ for normal displacements and pressure. The $H(\text{div})$ functions are constructed using a systematic methodology described in [12, 13].

2 GOVERNING EQUATIONS

In general elasticity, the governing equation of a continuum body $\Omega \in \mathbb{R}^3$ is given by:

$$-\nabla \cdot \boldsymbol{\sigma} - \mathbf{b} = \mathbf{0} \quad \text{in } \Omega, \quad (1)$$

where $\boldsymbol{\sigma}$ denotes the Cauchy stress tensor and \mathbf{b} is the body forces vector. For the well-posedness sake, proper boundary conditions need to be imposed on the Dirichlet boundary ($\partial\Omega_D$) and on the Neumann boundary ($\partial\Omega_N$), as said,

$$\mathbf{u} = \mathbf{u}_D \quad \text{on } \partial\Omega_D, \quad (2)$$

$$\boldsymbol{\sigma} \cdot \mathbf{n} = \mathbf{h} \quad \text{on } \partial\Omega_N. \quad (3)$$

The Generalized Hook law relates the stresses and strains by:

$$\boldsymbol{\sigma} = 2\mu\boldsymbol{\varepsilon} + \lambda\text{tr}(\boldsymbol{\varepsilon})\mathbf{I}, \quad (4)$$

where μ and λ are known as Lamé constants, $\boldsymbol{\varepsilon}$ is the infinitesimal strain tensor, computed as:

$$\boldsymbol{\varepsilon} = \frac{1}{2}(\nabla\mathbf{u}^T + \nabla\mathbf{u}), \quad (5)$$

and \mathbf{I} is the identity matrix. By recalling that the hydrostatic pressure is defined as

$$p = -\frac{\text{tr}(\boldsymbol{\sigma})}{3} = -\frac{(2\mu + \lambda)}{3}\text{tr}(\boldsymbol{\varepsilon}), \quad (6)$$

and considering that $\boldsymbol{\sigma} = \boldsymbol{\sigma}' - p\mathbf{I}$, Eq. (1) can be rewritten in a mixed form so the boundary-valued problem reads:

$$\begin{cases} -\nabla \cdot \boldsymbol{\sigma}'(\mathbf{u}) + \nabla p - \mathbf{b} = \mathbf{0} & \text{in } \Omega \\ -\nabla \cdot \mathbf{u} - \frac{1}{\kappa}p = 0 & \text{in } \Omega \\ \mathbf{u} = \mathbf{u}_D & \text{on } \partial\Omega_D \\ \boldsymbol{\sigma} \cdot \mathbf{n} = \mathbf{h} & \text{on } \partial\Omega_N \end{cases} \quad (7)$$

where $\kappa = \frac{2\mu+\lambda}{3}$ is the material bulk modulus, \mathcal{D}' is the fourth-order deviatoric part of the elasticity tensor and $\boldsymbol{\sigma}'$ refers to the deviatoric stress, computed as:

$$\boldsymbol{\sigma}' = 2\mu \left(\boldsymbol{\varepsilon} - \frac{1}{3} \text{tr}(\boldsymbol{\varepsilon}) \mathbf{I} \right). \quad (8)$$

One notices that when $\lambda \rightarrow \infty$, Eq. (7) recovers the classical mass conservation form of an incompressible material i.e. $\nabla \cdot \mathbf{u} = 0$.

3 WEAK FORM AND FINITE ELEMENT DISCRETIZATION

The variational form of Eqs. (7) can be obtained by means of the weighted residual method. Depending on the choice of test functions and approximation spaces, different formulations can be derived. We shall start from the most simplistic one, the primal displacement formulation and then move to the fully hybrid scheme.

Let $\mathcal{T} = \{\Omega_e, e = 1, \dots, n_e\}$ be a partition of Ω in n_e finite elements Ω_e with hexahedral shape for $d = 3$. The set \mathcal{E} contains all the element edges E and $\mathcal{E}_0 = \{E \in \mathcal{E} : E \subset \Omega\}$ denotes the internal edges or element interfaces. Let introduce the following function spaces:

3.1 Primal displacement formulation

The primal displacement formulation is obtained by multiplying Eq. (1) by test functions $\mathbf{v} \in \mathbf{V} | \mathbf{V} \subset H^1(\mathcal{T})$ and integrating over the discretized domain \mathcal{T} [14]. The weak statement reads: find $\mathbf{u} \in \mathbf{V}$ such that for all $\mathbf{v} \in \mathbf{V}$,

$$\sum_{\Omega_e \in \mathcal{T}} \int_{\Omega_e} \boldsymbol{\varepsilon}(\mathbf{u}) : \mathcal{D}' : \boldsymbol{\varepsilon}(\mathbf{v}) d\Omega_e = \sum_{\Omega_e \in \mathcal{T}} \left(\int_{\Omega_e} \mathbf{b} \cdot \mathbf{v} d\Omega_e + \int_{\Gamma_N} \mathbf{h} \cdot \mathbf{v} d\partial\Omega_e \right) \quad (9)$$

is satisfied. Although the primal displacement formulation is simple to implement, it has some limitations i.e. locking phenomena under bending and incompressibility. To overcome these limitations, we shall introduce the semi-hybrid formulation.

3.2 Semi-hybrid formulation

In [11], the authors proposed a semi-hybrid formulation for Stokes-Brinkman flows that uses $H(\text{div})$ conforming velocity functions and discontinuous L^2 approximation for pressure. The same idea can also be applied to elasticity. Let $\mathcal{V} = \mathbf{V} \cap H(\text{div}, \Omega)$, $\Psi \subset L^2(\Omega)$ be spaces of vector functions and piece-wise scalars, respectively, for which the relation $\nabla \cdot \mathcal{V} \in \Psi$ holds.

As $H(\text{div})$ approximation only guarantees the continuity of normal components of a vector across elements interface, a hybridization of the tangential velocity is performed. We introduce a third space defined as $\Lambda^t \subset H^{-1/2}(\partial\Omega_e)$, for which the Lagrange multiplier $\lambda^t \in \Lambda^t$ has the meaning of a shear traction to weakly enforce the tangential displacement continuity.

The weak statement for the semi-hybrid formulation thus reads: find $\{\mathbf{u}, p, \boldsymbol{\lambda}^t\} \in \mathcal{V} \times \Psi \times \Lambda^t$ such that for all $\mathbf{v}, q, \boldsymbol{\eta}^t \in \mathcal{V} \times \Psi \times \Lambda^t$:

$$\sum_{\Omega_e \in \mathcal{T}} \left(\int_{\Omega_e} \boldsymbol{\varepsilon}(\mathbf{v}) : \mathcal{D}' : \boldsymbol{\varepsilon}(\mathbf{u}) d\Omega_e + \int_{\Omega_e} p(\nabla \cdot \mathbf{v}) d\Omega_e + \int_{\mathcal{E}^0} \boldsymbol{\lambda}^t \cdot [\![\mathbf{v}]\!] d\partial\Omega_e \right) = \sum_{\Omega_e \in \mathcal{T}} \left(\int_{\Omega_e} \mathbf{v} \cdot \mathbf{f} d\Omega_e + \int_{\Gamma} \mathbf{v} \cdot \boldsymbol{\sigma}_N d\partial\Omega_e \right) \quad (10)$$

$$\sum_{\Omega_e \in \mathcal{T}} \left(- \int_{\Omega_e} (\nabla \cdot \mathbf{u}) q d\Omega_e - \int_{\Omega_e} \frac{3}{2\mu + \lambda} p q d\Omega_e \right) = \mathbf{0} \quad (11)$$

$$\sum_{\Omega_e \in \mathcal{T}} \int_{\mathcal{E}^0} [\![\mathbf{u}]\!] \cdot \boldsymbol{\eta}^t d\partial\Omega_e = \mathbf{0}, \quad (12)$$

where \mathbf{v} , q and $\boldsymbol{\eta}^t$ are test functions for velocity, pressure and tangential traction, respectively, $[\![\cdot]\!]$ stands for the jump operator on the interface \mathcal{E}^0 between two neighbour elements Ω_1 and Ω_2 , defined as $[\![\mathbf{v}]\!] = \mathbf{v}|_{\Omega_1} - \mathbf{v}|_{\Omega_2}$. Equation (12) plays the role of weakly enforcing the tangential displacement continuity over the element interfaces.

3.3 Fully hybrid formulation

Although mathematically consistent, the semi-hybrid formulation poses some challenges from a numerical perspective. It gives rise to a saddle-point problem with two different constraints: p and $\boldsymbol{\lambda}^t$. This structure significantly increases the efforts required to consistently and stably solve the linear system.

We propose a second hybridization of the tangential stresses in order to recover its primal form. Introducing the space $\mathcal{L}^t \subset H^{1/2}(\partial\Omega_e)$ for the tangential velocity, the hybrid form thus reads: find $\{\mathbf{u}, p, \boldsymbol{\lambda}, \mathbf{u}^t\} \in \mathcal{V} \times \Psi \times \Lambda^t \times \mathcal{L}^t$ such that for all $\mathbf{v}, q, \boldsymbol{\eta}, \mathbf{v}^t \in \mathcal{V} \times \Psi \times \Lambda^t, \mathcal{L}^t$, the following equations are satisfied:

$$\sum_{\Omega_e \in \mathcal{T}} \left(\int_{\Omega_e} \boldsymbol{\varepsilon}(\mathbf{v}) : \mathcal{D}' : \boldsymbol{\varepsilon}(\mathbf{u}) d\Omega_e + \int_{\Omega_e} p(\nabla \cdot \mathbf{v}) d\Omega_e + \int_{\partial\Omega_e} \boldsymbol{\lambda}^t \cdot \mathbf{v} d\partial\Omega_e \right) = \sum_{\Omega_e \in \mathcal{T}} \left(\int_{\Omega_e} \mathbf{v} \cdot \mathbf{f} d\Omega_e + \int_{\Gamma} \mathbf{v} \cdot \boldsymbol{\sigma}_N d\partial\Omega_e \right) \quad (13)$$

$$\sum_{\Omega_e \in \mathcal{T}} \left(- \int_{\Omega_e} (\nabla \cdot \mathbf{u}) q d\Omega_e - \int_{\Omega_e} \frac{3}{2\mu + \lambda} p q d\Omega_e \right) = \mathbf{0} \quad (14)$$

$$\sum_{\Omega_e \in \mathcal{T}} \left(\int_{\partial\Omega_e} \mathbf{u} \cdot \boldsymbol{\eta}^t d\partial\Omega_e + \int_{\mathcal{E}^0} [\![\boldsymbol{\eta}^t]\!] \cdot \mathbf{u}^t d\partial\Omega_e \right) = \mathbf{0} \quad (15)$$

$$\sum_{\Omega_e \in \mathcal{T}} \int_{\mathcal{E}^0} [\![\boldsymbol{\lambda}^t]\!] \cdot \mathbf{v}^t d\partial\Omega_e = \mathbf{0}, \quad (16)$$

where Eq. (16) was introduced to impose the continuity of the tangential traction across \mathcal{E}^0 . Even though an additional constraint is introduced, $\boldsymbol{\lambda}^t$ is now associated to a single element therefore it can be statically condensed and eliminated from the global system. For a compressible solid, a symmetric positive-definite matrix is obtained with two unknowns, namely \mathbf{u} and \mathbf{u}^t . For the incompressible case where pressures cannot be computed explicitly from the displacements, one mean pressure per element must be left in the global system. This still gives rise to a saddle-point matrix, however, with much better spectral properties and easier to solve compared to Eqs. (10)-(12).

4 NUMERICAL EXAMPLES

This Section presents two examples to verify the primal hybrid formulation. The first one is a cantilever beam subjected to an end shear load, where a convergence test is carried out and compared to the analytical solution. The second example is a practical application where the proposed method was used to simulate a real structural casket used to run experimental analysis on petroleum engineering.

4.1 Cantilever beam subjected to an end shear load

Figure 1a shows a cantilever beam where $L = 5$, $a = 0.5$ and $b = 0.5$. The beam is assumed to be fixed at $z = 0$ and subjected to an unitary shear-force $F = \int_{-b}^b \int_{-a}^a \sigma_{yz} dx dy = 1$ at $z = L$. The Young modulus is $E = 1$ and different values for the poisson coefficient is used to test the formulation in different compressibility regimes, i.e. $\nu = 0.3$, $\nu = 0.4999$ and $\nu = 0.5$.

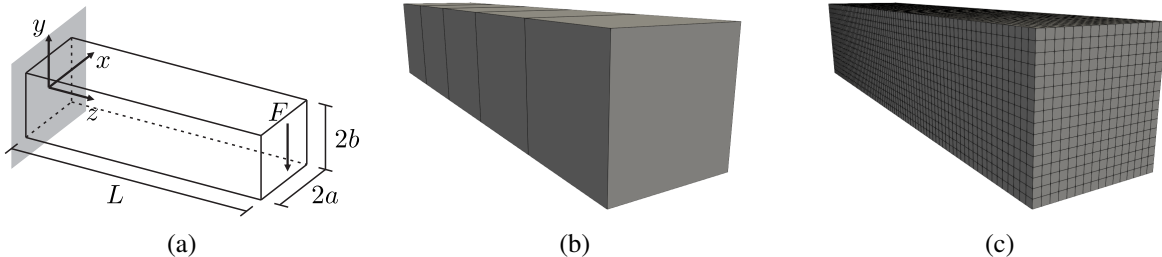


Figure 1: Cantilever beam subjected to an end shear load - geometry (at left), coarsest mesh (at center) and finest mesh (at right)

The analytical solutions for the stresses and displacements are available in [15] and written below:

$$\begin{aligned}
 \sigma_{xx} &= \sigma_{xy} = \sigma_{yy} = 0, \\
 \sigma_{zz} &= \frac{F}{I} yz, \\
 \sigma_{xz} &= \frac{F}{I} \frac{2a^2}{\pi^2} \frac{\nu}{1+\nu} \sum_{n=1}^{\infty} \frac{(-1)^n}{n^2} \sin(n\pi x/a) \frac{\sinh(n\pi y/a)}{\cosh(n\pi b/a)}, \\
 \sigma_{yz} &= \frac{F}{I} \frac{b^2 - y^2}{2} + \frac{F}{I} \frac{\nu}{1+\nu} \left[\frac{3x^2 - a^2}{6} - \frac{2a^2}{\pi^2} \sum_{n=1}^{\infty} \frac{(-1)^n}{n^2} \cos(n\pi x/a) \frac{\cosh(n\pi y/a)}{\cosh(n\pi b/a)} \right],
 \end{aligned} \tag{17}$$

and

$$\begin{aligned}
 u_x &= -\frac{F\nu}{EI} xyz, \\
 u_y &= \frac{F}{EI} \left[\frac{\nu}{2} (x^2 - y^2) z - \frac{1}{6} z^3 \right], \\
 u_z &= \frac{F}{EI} \left[\frac{1}{2y} (\nu x^2 + z^2) z + \frac{1}{6} \nu y^3 + (1+\nu) \left(b^2 y - \frac{1}{3} y^3 \right) - \frac{1}{3} a^2 \nu y \right. \\
 &\quad \left. - \frac{4a^3 \nu}{\pi^3} \sum_{n=1}^{\infty} \frac{(-1)^n}{n^3} \cos(n\pi x/a) \frac{\sinh(n\pi y/a)}{\cosh(n\pi b/a)} \right].
 \end{aligned} \tag{18}$$

where $I = 4ab^3/3$ is the second moment of area about the x -axis, and the series above are evaluated with a finite number of terms $n = 5$.

The beam is discretized using hexahedral elements, where the element size is computed as $h_e = 1/2^N$, with $N = \{0, 1, 2, 3, 4\}$. The coarsest ($h_e = 1$) and finest ($h_e = 0.0625$) meshes are shown in Figures 1b-1c. A convergence test is performed for displacement, pressure, stress and mass conservation, where the error is computed according to the L^2 norm defined as:

$$\|\mathbf{u}^h - \mathbf{u}_{exact}\|_{L^2} \doteq \left[\sum_{e=1}^n \int_{\Omega_e} (\mathbf{u} - \mathbf{u}^h)^2 d\Omega_e \right]^{1/2}. \tag{19}$$

The results are depicted in Figures 2-4 and present optimal convergence rates of $k+1$ for the displacement and k for the remaining variables independently of the poisson coefficient. This is a nice feature as many formulations present a locking phenomena under quasi and full incompressibility. For the incompressible case ($\nu = 0.5$), a divergence free displacement field is obtained even for the coarsest mesh thanks to the stable pair $H(\text{div}, \Omega)$ - $L^2(\Omega)$, with the error bounded to the machine precision.

Figure 5 plots the displacement, pressure, normal and shear stresses distributions obtained with the finest mesh using $k = 2$ over the deformed configuration of the beam for the compressible case. The results qualitatively agrees with the reference solution of [15].

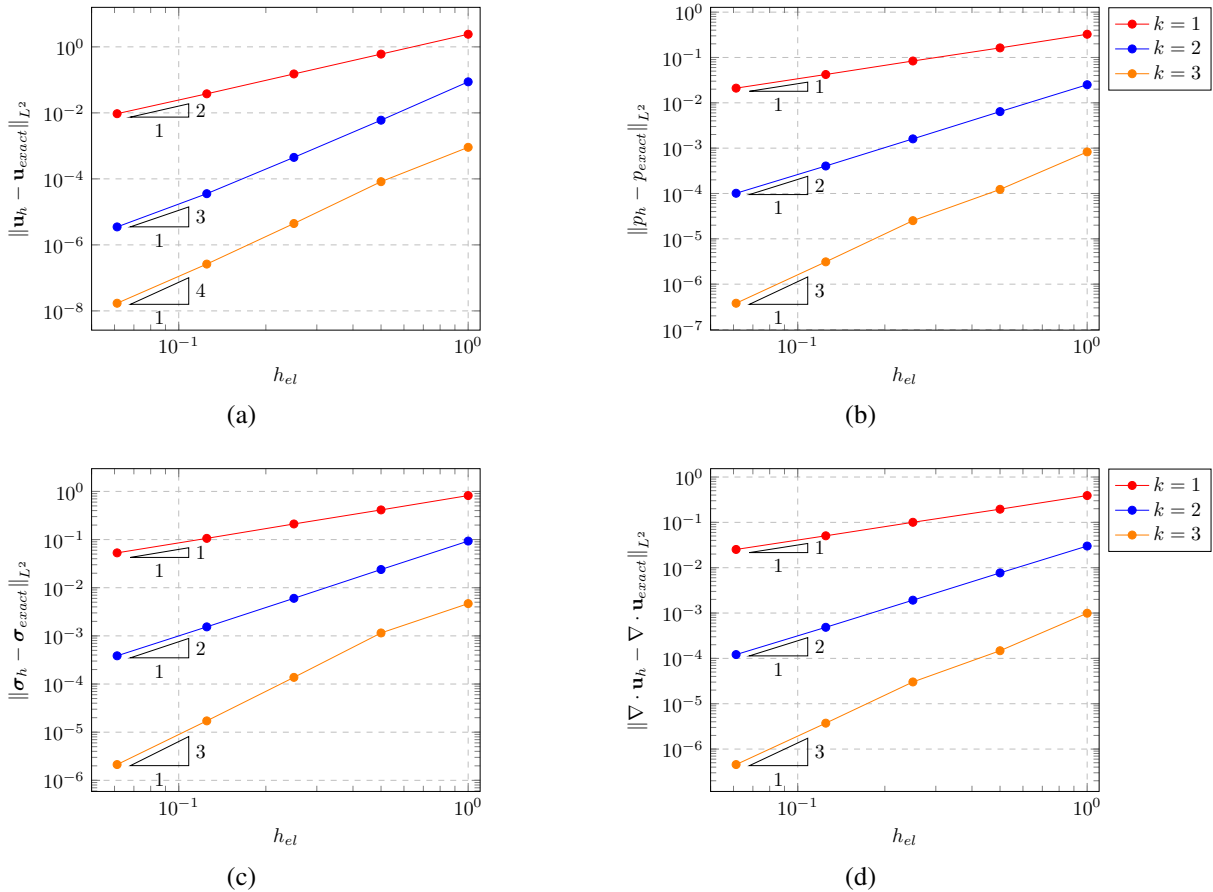


Figure 2: Cantilever beam subjected to an end shear load - convergence analysis for the compressible case ($\nu = 0.30$)

4.2 Experimental apparatus used in petroleum engineering

The second example consists on a thin-walled structural casket that is subjected to an internal pressure load due to the filling of saturated sand. This is a real apparatus designed to run experimental analyses of the loss of injectivity of produced water in petroleum wellbores, financed by Total Energies. The hull is made of steel, with Young modulus $E = 210 \times 10^3$ MPa, poisson coefficient $\nu = 0.3$, thickness $t = 45.1$ mm, internal radius $R_i = 344.9$ mm and length $L = 1000$ mm. The internal pressure is assumed to be $p = 10.34$ MPa. A real picture of the module is shown in Figure 6a. The Von Mises stress and displacement fields are plotted in Figures 6b-6c. From a qualitatively point of view, the results are in agreement with the expected physics of the problem.

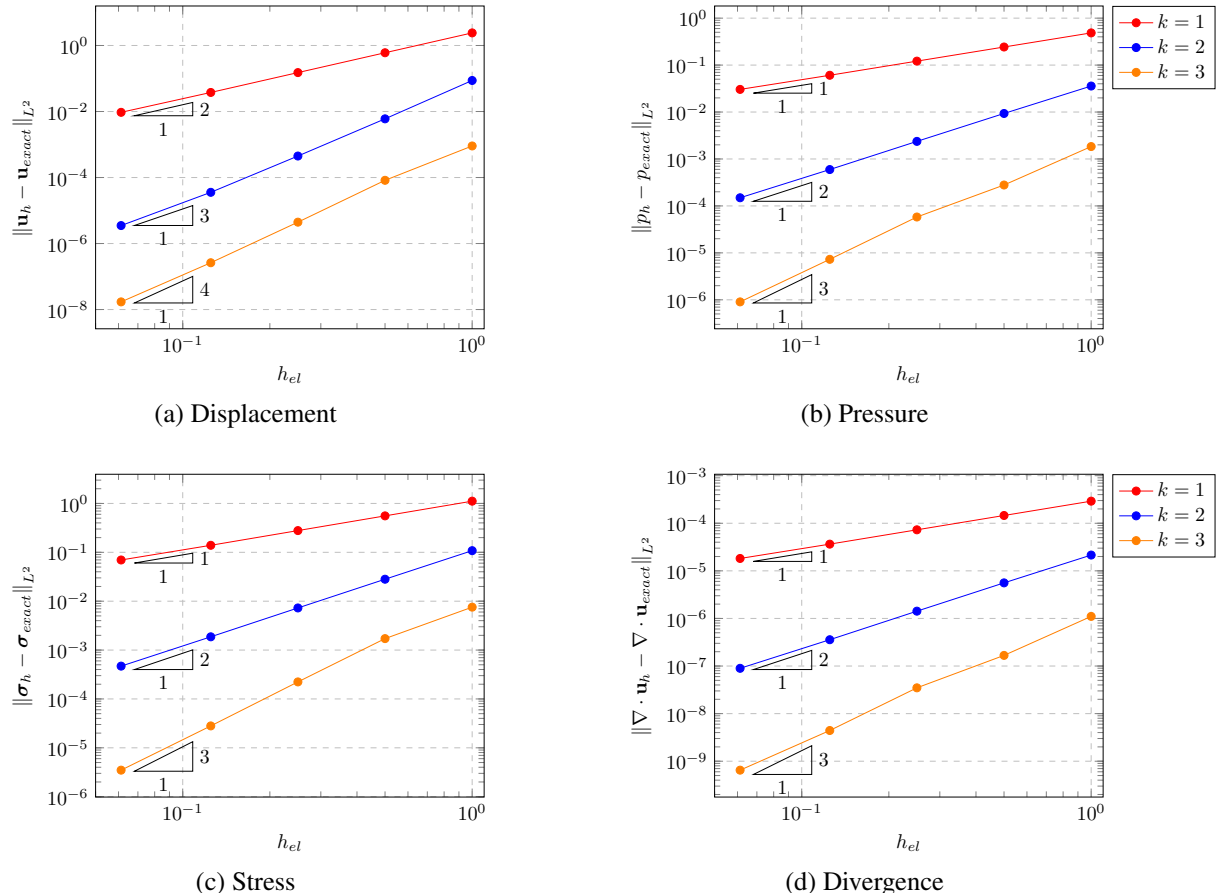


Figure 3: Cantilever beam subjected to an end shear load - convergence analysis for the quasi-incompressible case ($\nu = 0.4999$)

5 CONCLUSIONS

In this work we developed a primal hybrid formulation for tridimensional elasticity problems. The approximation space composed of $H(\text{div})$ functions for the normal displacements and L^2 functions for the pressure leads to a locally conservative scheme as it is De Rham compatible. The second hybridization of the tangential stresses was done in order to make possible their elimination of the global system by applying a static condensation. This leads to a symmetric positive-definite matrix when analysing compressible solids and a saddle point problem with a single mean pressure per element for incompressible materials.

The formulation was tested for a cantilever beam subjected to an end shear load and the results showed optimal convergence rates of $k + 1$ for the displacement and k for the remaining variables independently of the poisson coefficient. The formulation was able to capture the correct stress and displacement distributions for the compressible case and a divergence free displacement field for the incompressible case. The simulation of the real scale structural hull

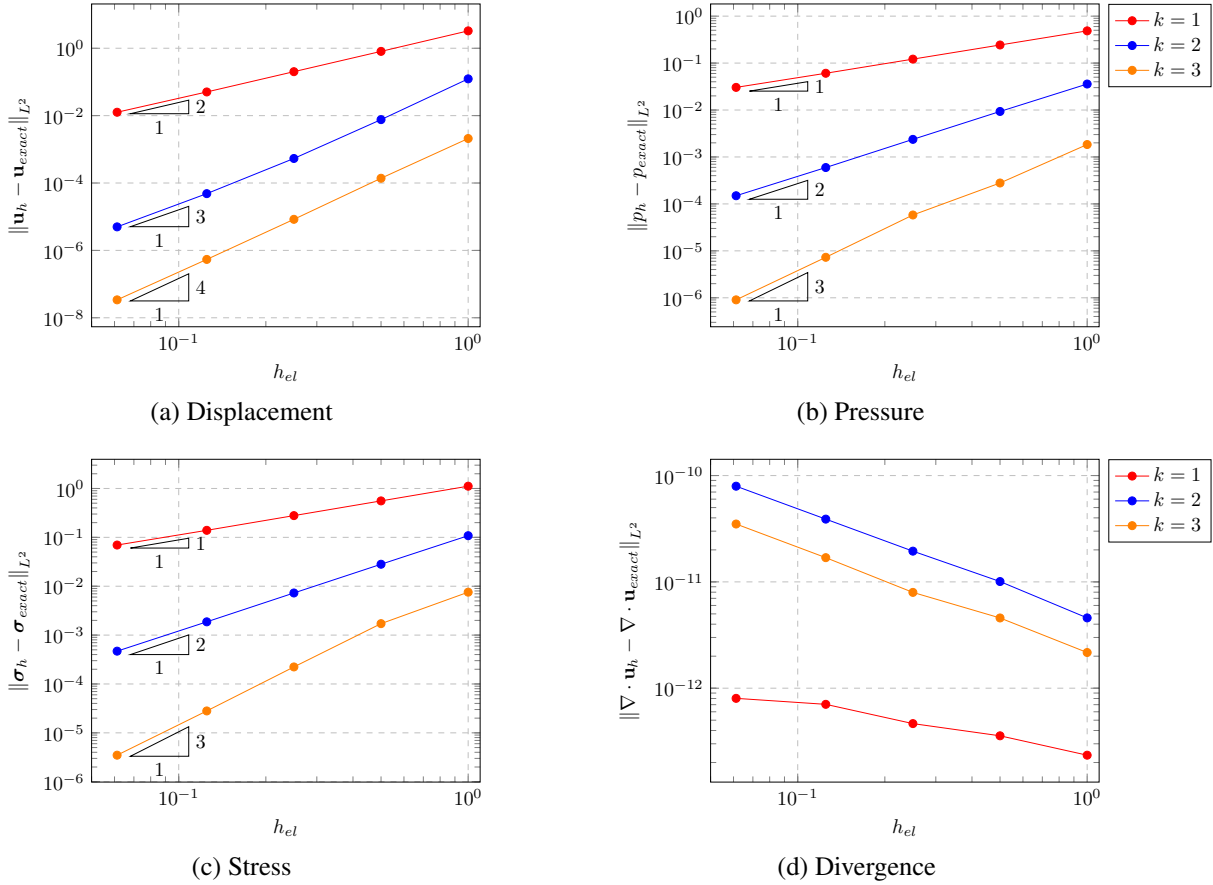


Figure 4: Cantilever beam subjected to an end shear load - convergence analysis for the incompressible case ($\nu = 0.5$)

subjected to an internal pressure qualitatively indicates that the proposed method could be applied to real engineering problems.

Acknowledgements. We gratefully acknowledge the support of EPIC - Energy Production Innovation Center through FAPESP/Equinor (Grant 2023/06981/5), Total Energies Brazil through FUNCAMP (Process 76042-23) and the Brazilian National Council for Scientific and Technological Development (grants 305823/2017-5 and 309597/2021-8). We also acknowledge the support of ANP (Brazil's National Oil, Natural Gas and Biofuels Agency).

REFERENCES

- [1] K.-U. Bletzinger, M. Bischoff, and E. Ramm, “A unified approach for shear-locking-free triangular and rectangular shell finite elements,” *Computers & Structures*, vol. 75, no. 3,

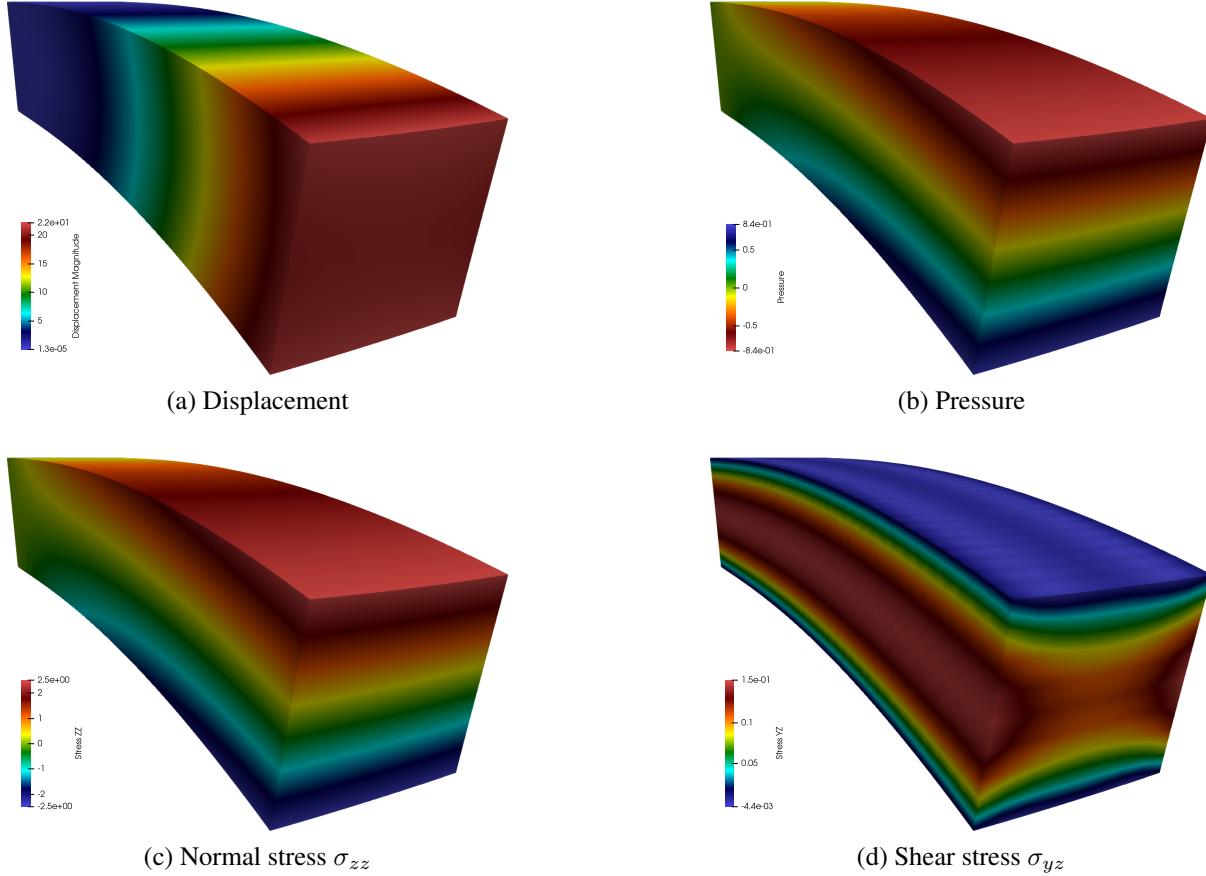


Figure 5: Cantilever beam subjected to an end shear load - snapshots for $\nu = 0.3$

pp. 321–334, 2000.

- [2] T. Belytschko, H. Stolarski, W. K. Liu, N. Carpenter, and J. S. Ong, “Stress projection for membrane and shear locking in shell finite elements,” *Computer Methods in Applied Mechanics and Engineering*, vol. 51, no. 1-3, pp. 221–258, 1985.
- [3] E. D. S. Neto, F. A. Pires, and D. Owen, “F-bar-based linear triangles and tetrahedra for finite strain analysis of nearly incompressible solids. part i: formulation and benchmarking,” *International Journal for Numerical Methods in Engineering*, vol. 62, no. 3, pp. 353–383, 2005.
- [4] M. Cervera, M. Chiumenti, Q. Valverde, and C. A. de Saracibar, “Mixed linear/linear simplicial elements for incompressible elasticity and plasticity,” *Computer Methods in Applied Mechanics and Engineering*, vol. 192, no. 49-50, pp. 5249–5263, 2003.

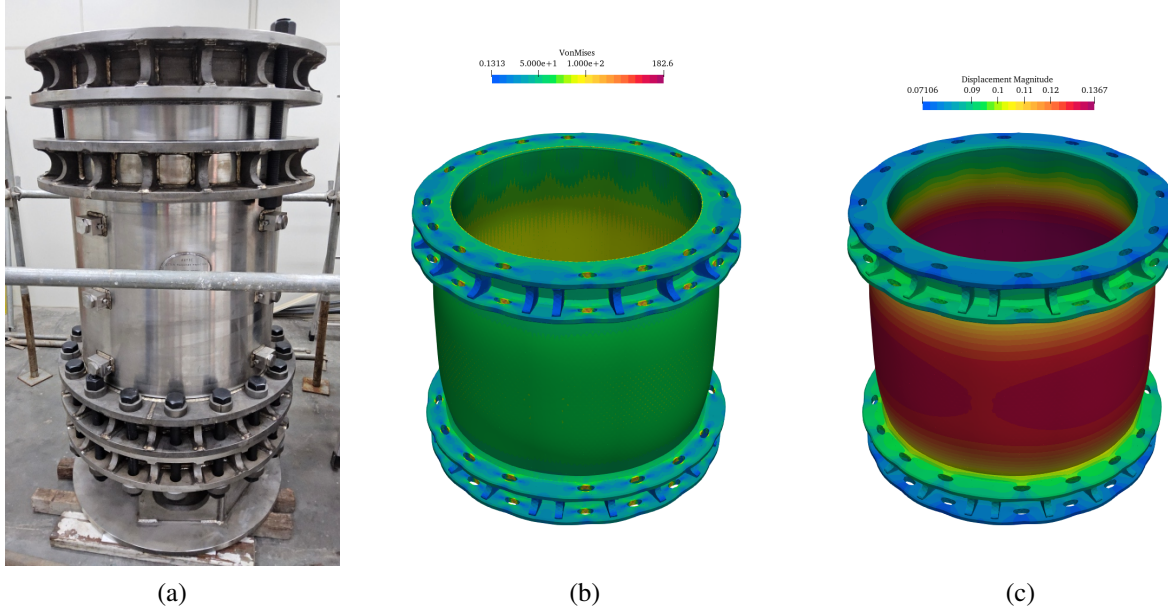


Figure 6: Structural casket subjected to an internal pressure load - real apparatus (at left) and simulation results (Von Mises stress at center and displacement at right)

- [5] F. Brezzi and M. Fortin, *Mixed and hybrid finite element methods*, vol. 15. Springer Science & Business Media, 2012.
- [6] D. N. Arnold and R. S. Falk, “A new mixed formulation for elasticity,” *Numerische Mathematik*, vol. 53, no. 1, pp. 13–30, 1988.
- [7] C. Taylor and P. Hood, “A numerical solution of the navier-stokes equations using the finite element technique,” *Computers & Fluids*, vol. 1, no. 1, pp. 73–100, 1973.
- [8] P.-A. Raviart and J.-M. Thomas, “Primal hybrid finite element methods for 2nd order elliptic equations,” *Mathematics of computation*, vol. 31, no. 138, pp. 391–413, 1977.
- [9] C. Harder, A. L. Madureira, and F. Valentin, “A hybrid-mixed method for elasticity,” *ESAIM: Mathematical Modelling and Numerical Analysis*, vol. 50, no. 2, pp. 311–336, 2016.
- [10] M. Farhloul and M. Fortin, “Dual hybrid methods for the elasticity and the stokes problems: a unified approach,” *Numerische Mathematik*, vol. 76, pp. 419–440, 1997.
- [11] P. G. Carvalho, P. R. Devloo, and S. M. Gomes, “A semi-hybrid-mixed method for stokes–brinkman–darcy flows with h (div)-velocity fields,” *International Journal for Numerical Methods in Engineering*, vol. 125, no. 1, p. e7363, 2024.

- [12] P. R. Devloo, J. W. Fernandes, S. M. Gomes, F. T. Orlandini, and N. Shauer, “An efficient construction of divergence-free spaces in the context of exact finite element de rham sequences,” *Computer Methods in Applied Mechanics and Engineering*, vol. 402, p. 115476, 2022.
- [13] D. De Siqueira, P. R. Devloo, and S. M. Gomes, “A new procedure for the construction of hierarchical high order hdiv and hcurl finite element spaces,” *Journal of Computational and Applied Mathematics*, vol. 240, pp. 204–214, 2013.
- [14] E. Becker, G. Carey, and J. Oden, “Finite elements: An introduction,” no. v. 1, 1981.
- [15] J. E. Bishop, “A displacement-based finite element formulation for general polyhedra using harmonic shape functions,” *International Journal for Numerical Methods in Engineering*, vol. 97, no. 1, pp. 1–31, 2014.